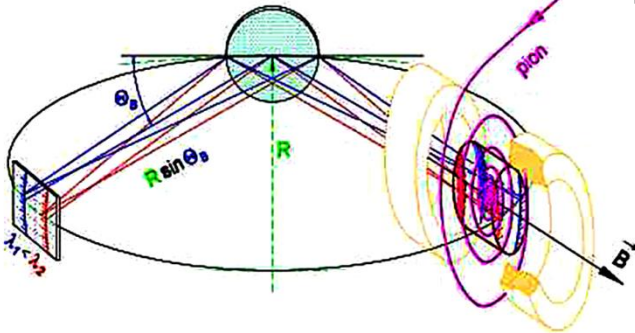


# ***CCDs - a Swiss Army knife for low-energy experiments***

*Mihail Antoniu Iliescu,  
Fundamental physics with exotic atoms and radiation detectors,  
INFN-LNF, Frascati, November 2021*

# Scientific CCDs

High QE, high res position detectors



CCDs, Bragg lens and cyclotron trap

**Antiprotonic hydrogen and deuterium**  
(two-arm) M. Augsburger et al, Nucl. Phys. A 658, 149 (1999). **Pion mass** S. Lenz et al. Ph. Lett. B 416, 50 (1998). **Pion deuterium** D. Chatellard et al., Phys. Rev. Lett. 74, 4157 (1995).

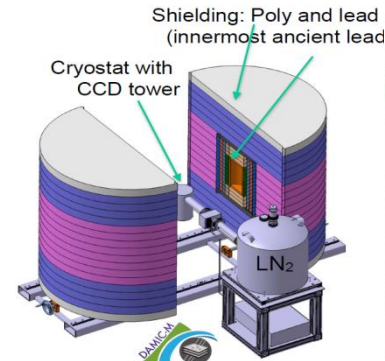
High QE, high E-res direct spectroscopy Event ID by topology & energy Fast, high res, rad hard



CCDs for **Muonic Hydrogen** B. Lauss et al Phys. Rev. Lett. 80(14) 1997

CCDs in **DEAR Kaonic Hydrogen** G. Beer et al PRL 94, 212302 (2005)

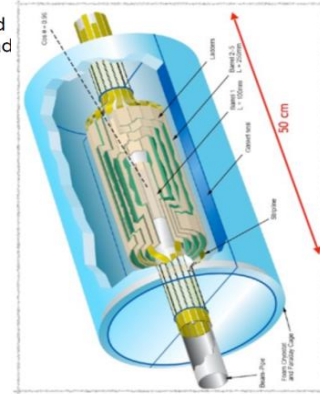
CCDs in **VIP (PEP violation limit)** S. Bartalucci et al Phys. Lett. B 641 (2006)



CCDs in **DAMIC**

**Dark matter search**

A. Aguilar-Arevalo et al Phys. Rev. Lett. 125 (2020).



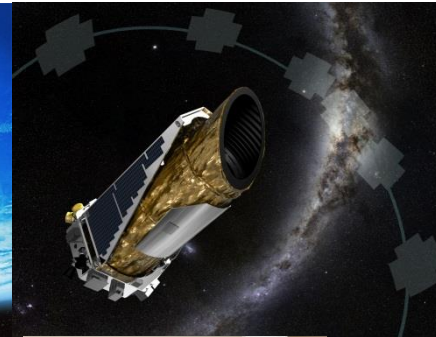
CCDs at **LCFI as vertex detectors** (fast parallel readout) A. Sopczak et al JINST 3 P05007 2008



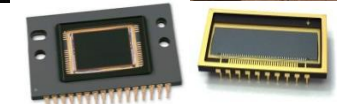
**Hubble CCD**  
Teledyne-E2V  
1990



**EPIC CCDs XMM Newton 1999**  
Xray from 0.15 to 15 keV



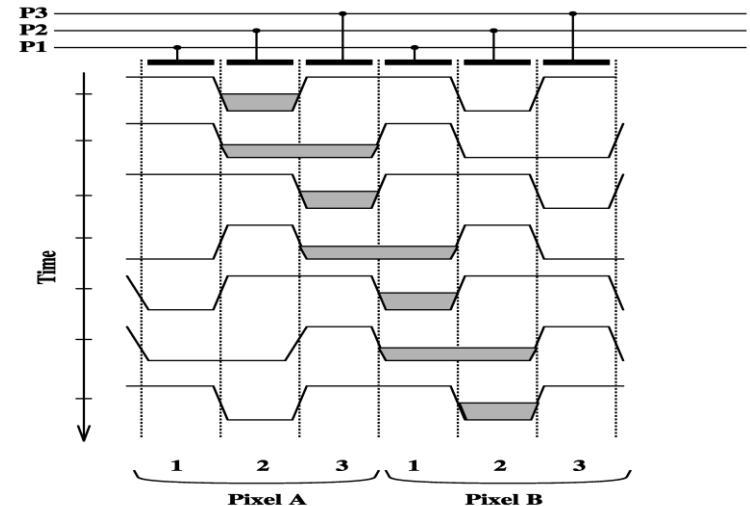
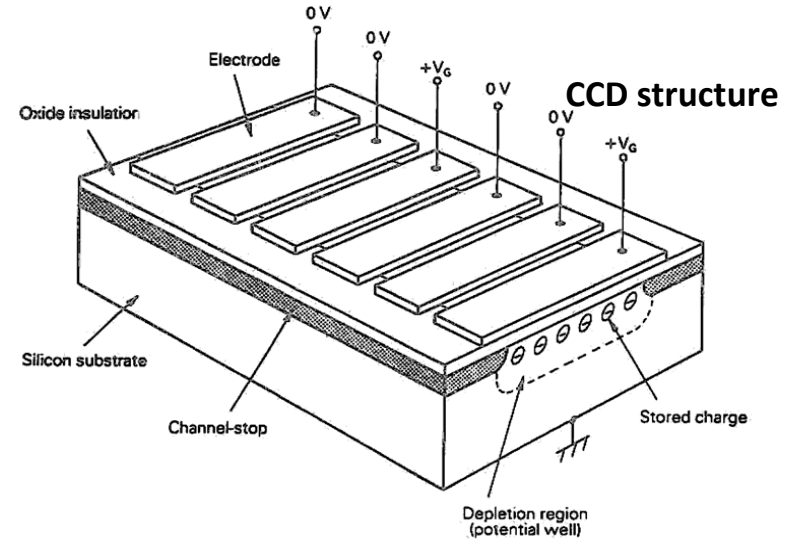
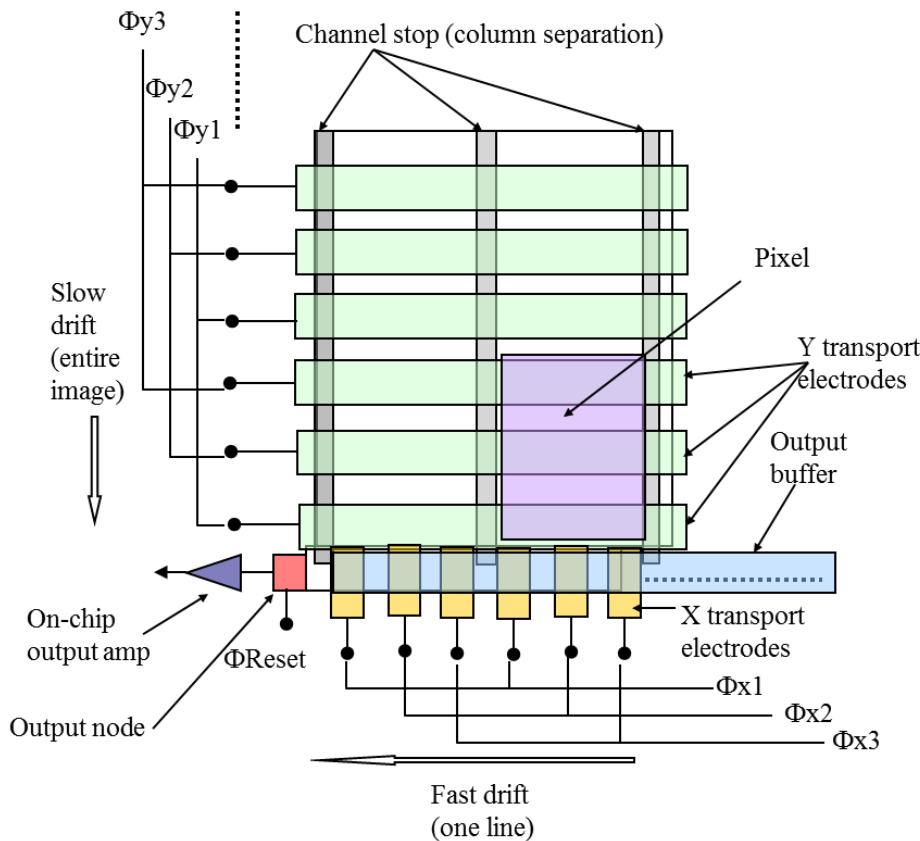
**Kepler CCD array 2009**



**Perseverance 2021 MAST**  
(main cam-ONSEMI KAI2020 CCD)  
**SHERLOC & SuperCam**  
(laser Raman/fluor/time resolved  
Teledyne-E2V CCD42-10)

# Working principle of CCDs

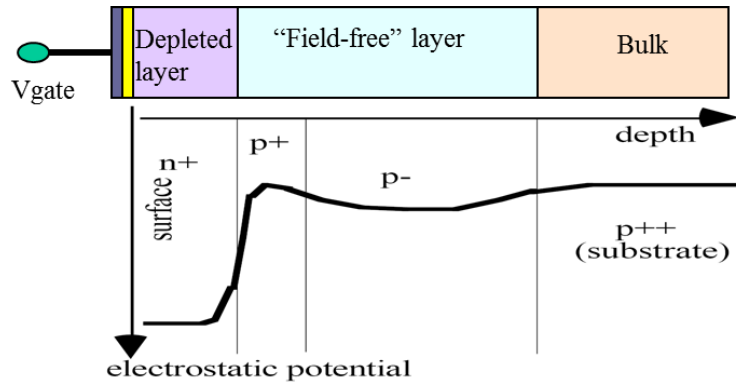
The CCDs (1969 at Bell Labs by Willard Boyle and George Smith) are MOS imaging devices in which the pixels are a combination of a light sensitive diode and a capacitor for charge storage.



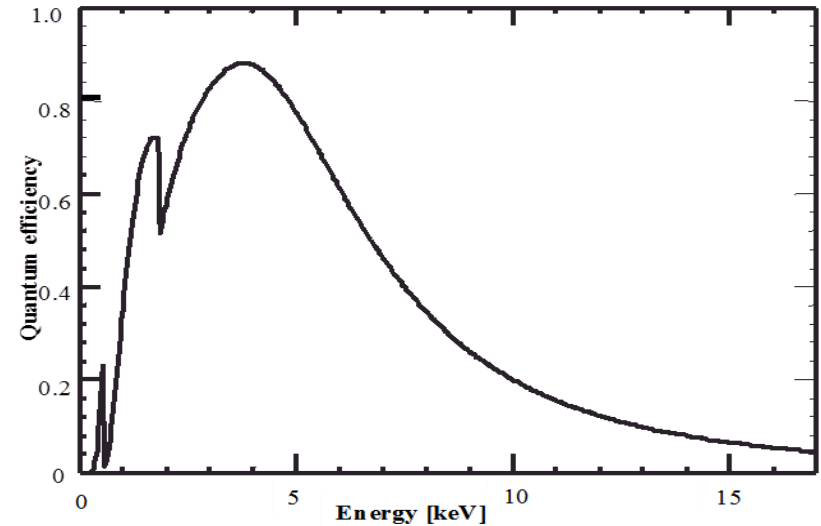
Charge packet transport with three-phase modulated field

**General architecture of a CCD.**  $\Phi 1-3$  represent the three-phase voltages used for the charge collection and transport, applied on x and y electrodes.  $\Phi$  reset is the voltage used for emptying the node before each pixel packet comes in.

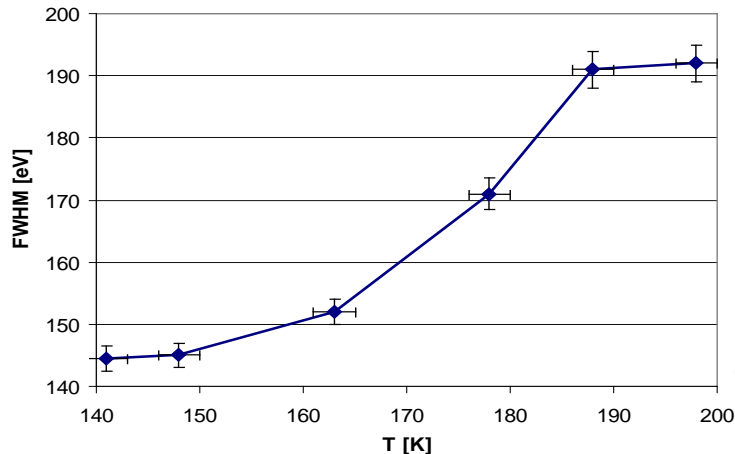
# Working principle of CCDs



Cross section of a CCD pixel showing the potential well created by doping concentration and the applied field.



Quantum efficiency for 30  $\mu\text{m}$  depleted silicon

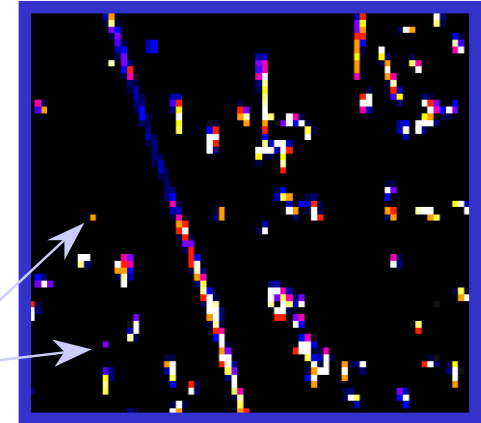
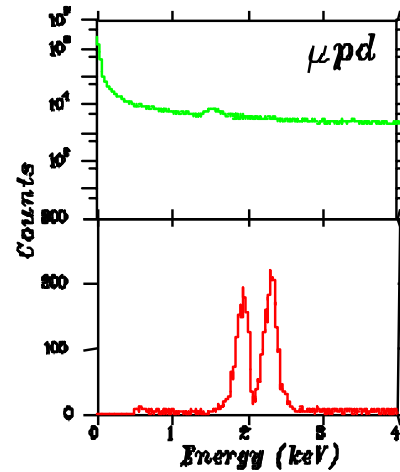
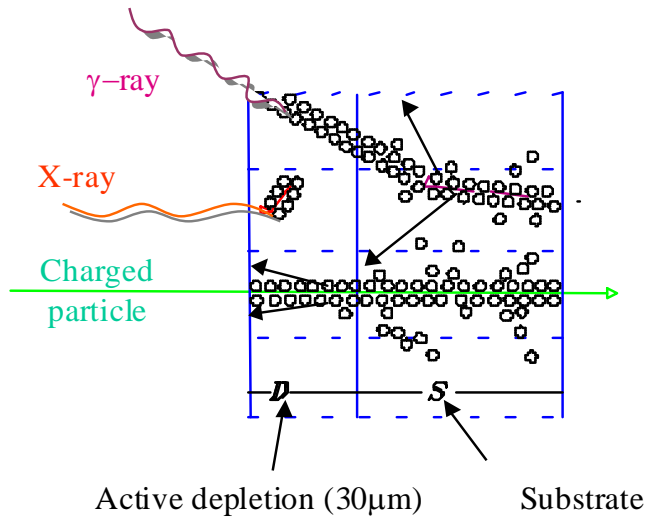


Energy resolution given by Fano formula:

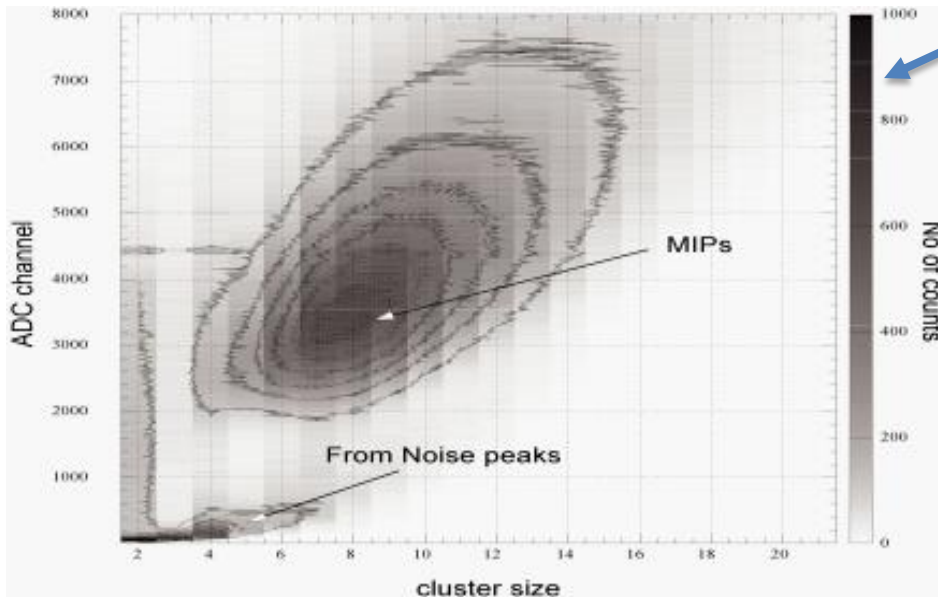
$$\Delta E = \omega \cdot \sqrt{n^2 + \frac{FE}{\omega}}$$

FWHM for the Mn  $K_{\alpha}$  (5.9 KeV) line as a function of temperature (INFN-LNF, 2000)

# X-ray spectroscopy with CCDs in high radiation environment



**Background suppression by single pixel selection**



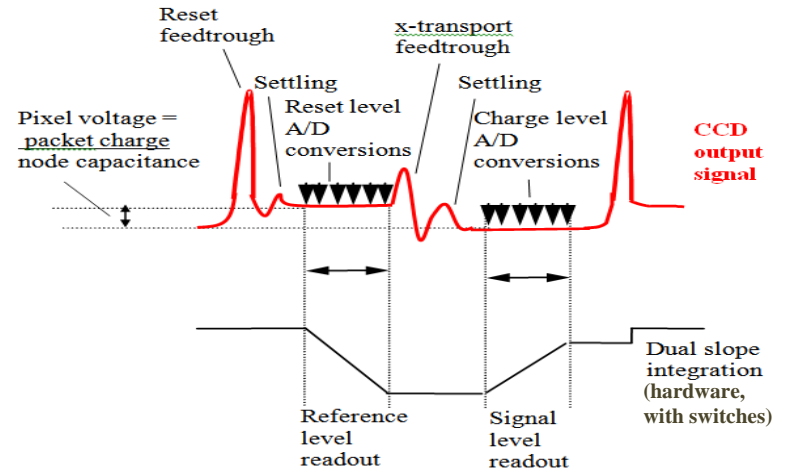
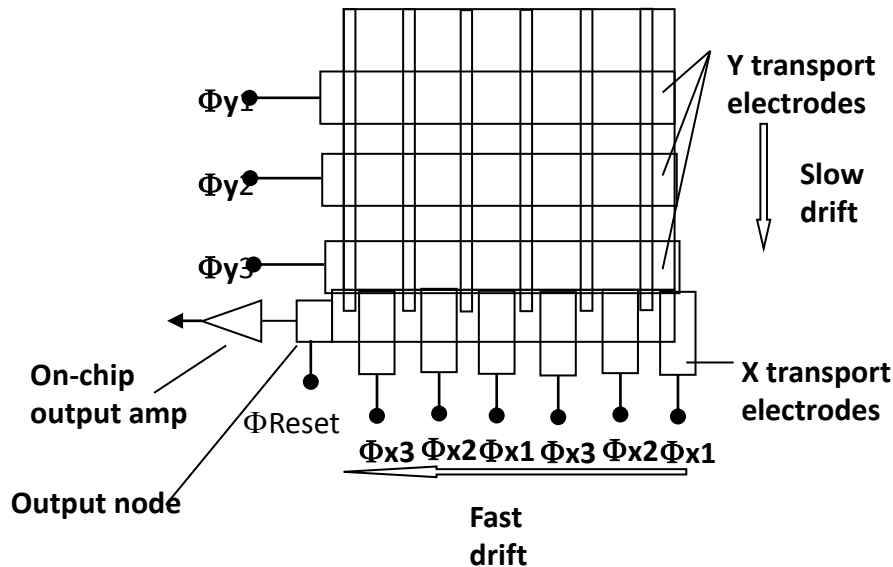
**Limitation:** geometric efficiency drops as a function of occupancy. For the cluster size distribution obtained in DAFNE:

Occupancy	Efficiency
6%	>99%
15%	75%
29%	61%
36%	49%
44%	29%

**Drives the max single exposure time**



# CCDs readout procedure



CCD signal output with correlated double sampling

9	10	11	12	13
14	8	1	5	15
16	3	X	4	17
18	7	2	6	19
20	21	22	23	24

Grade 0

- Charge transport into the CCD output node (lines, columns)
- software dual slope integration (correlated double sampling);

in-pixel noise cut  
last bit of conversion exact  
cable pickup noise eliminated  
integrator control (duration, band)  
no switch noise

Other features:

- data compression and saving
- Collider injection synchronization (reset)

9	10	11	12	13
14	8	1	5	15
16	3	X	4	17
18	7	2	6	19
20	21	22	23	24

Grade 1

9	10	11	12	13
14	8	1	5	15
16	3	X	4	17
18	7	2	6	19
20	21	22	23	24

Grade 2

9	10	11	12	13
14	8	1	5	15
16	3	X	4	17
18	7	2	6	19
20	21	22	23	24

Grade 3

9	10	11	12	13
14	8	1	5	15
16	3	X	4	17
18	7	2	6	19
20	21	22	23	24

Grade 4

9	10	11	12	13
14	8	1	5	15
16	3	X	4	17
18	7	2	6	19
20	21	22	23	24

Grade 5

9	10	11	12	13
14	8	1	5	15
16	3	X	4	17
18	7	2	6	19
20	21	22	23	24

Grade 6

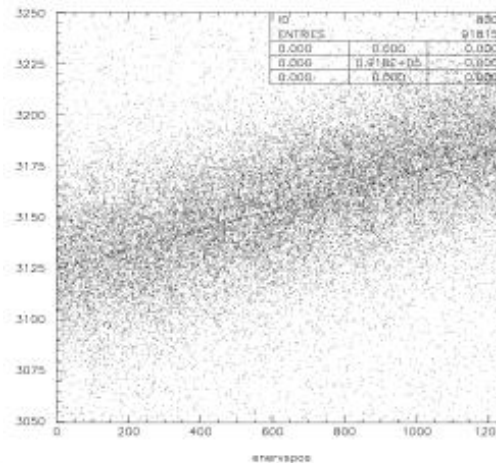
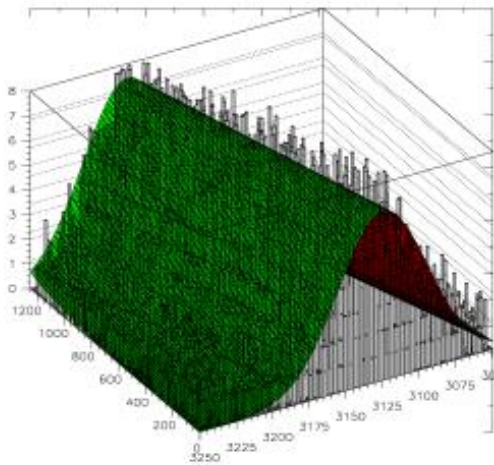
9	10	11	12	13
14	8	1	5	15
16	3	X	4	17
18	7	2	6	19
20	21	22	23	24

Grade 7

9	10	11	12	13
14	8	1	5	15
16	3	X	4	17
18	7	2	6	19
20	21	22	23	24

Grade 8

# CCD charge transport correction and EMI noise filtering

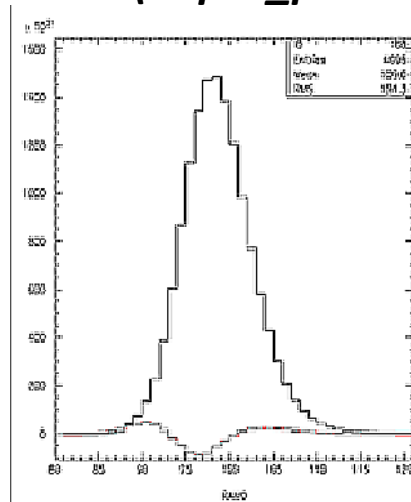


Zr K<sub>α</sub> peak position versus X pixel coordinate and the charge transport correction function

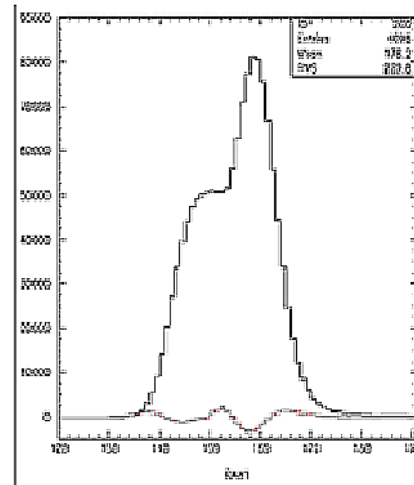
$$Q_{final} = Q_{initial} - X_{pixel} * C1 * Q_{initial}^{C2}$$

**Fast EMI noise injection estimator**

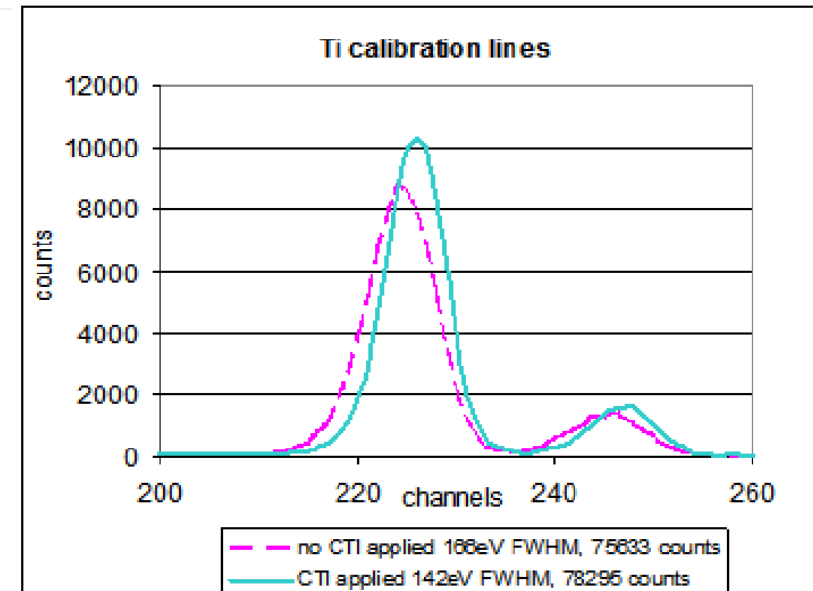
$$F = (d2pos\_peaks - 2) + (d2neg\_peaks - 1)$$



**F=0**



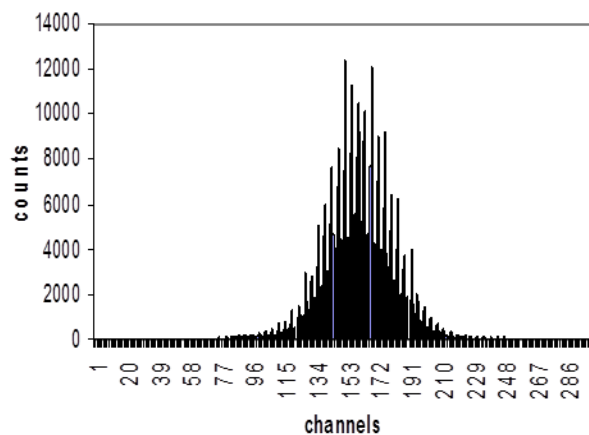
**F=2**



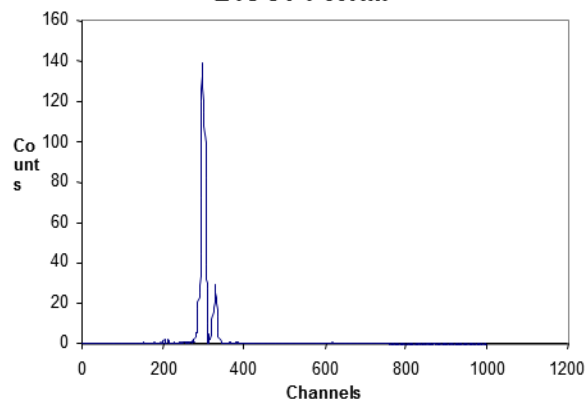
Effect of charge transport correction on Ti K<sub>α</sub> calibration line (4.51 keV)

# Progress in CCD readout reached by the DEAR group (new CCD type, new amplifier, new DAQ system)

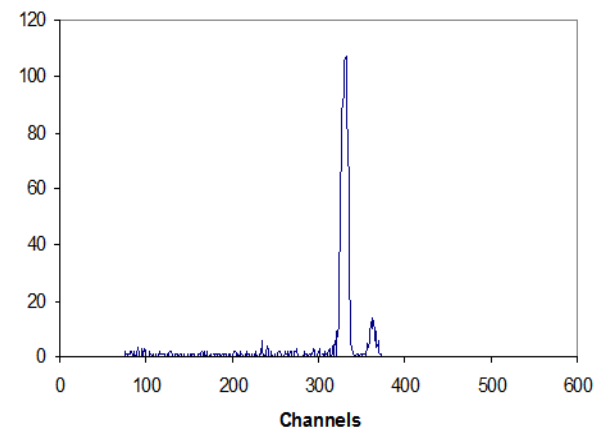
Thermal noise ccd22 old electronics



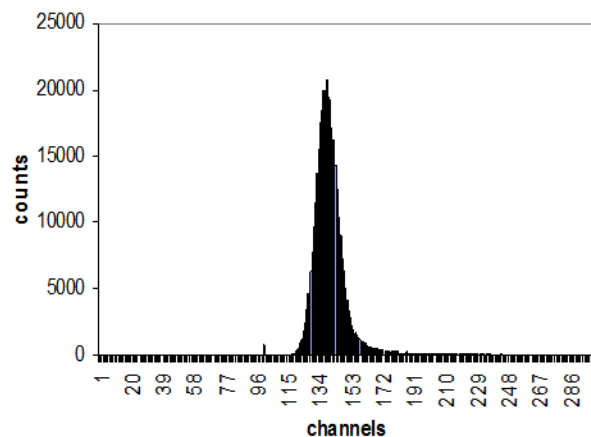
CCD 22 old DAQ Mn  $K_{\alpha}$   $K_{\beta}$   
215 eV FWHM



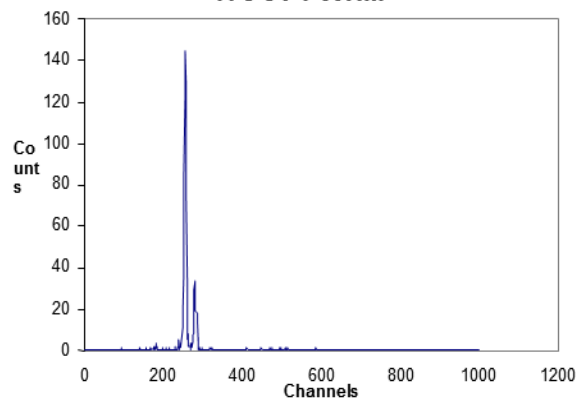
CCD 55 new DAQ old amp Mn  $K_{\alpha}$   $K_{\beta}$   
145 eV FWHM



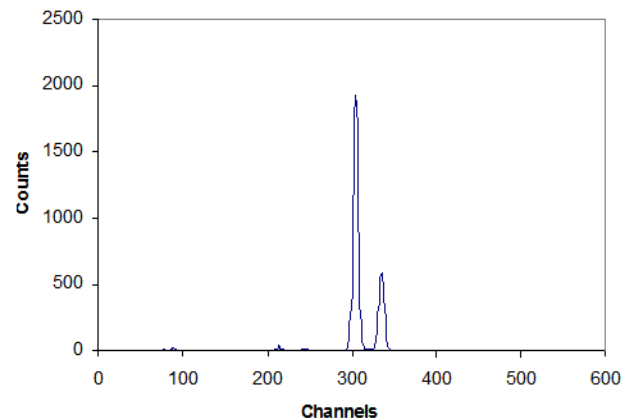
Thermal noise ccd22 new electronics



CCD22 new DAQ Mn  $K_{\alpha}$   $K_{\beta}$   
173 eV FWHM

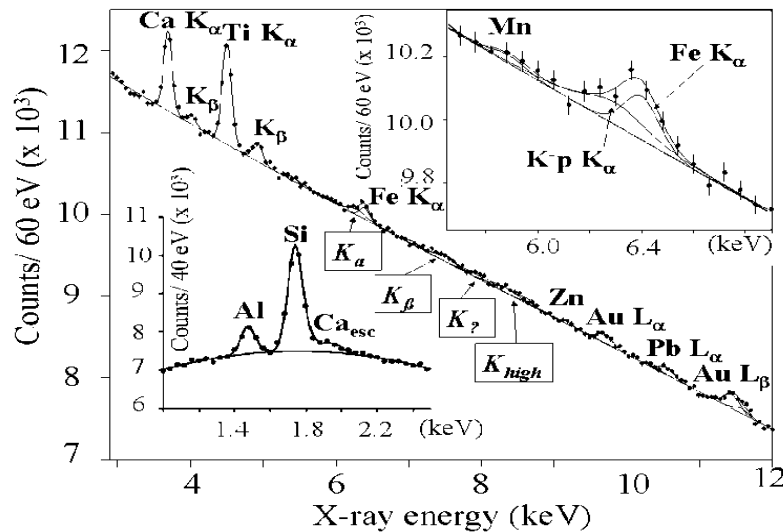


CCD55 new DAQ new amp Mn  $K_{\alpha}$   $K_{\beta}$   
136 eV FWHM



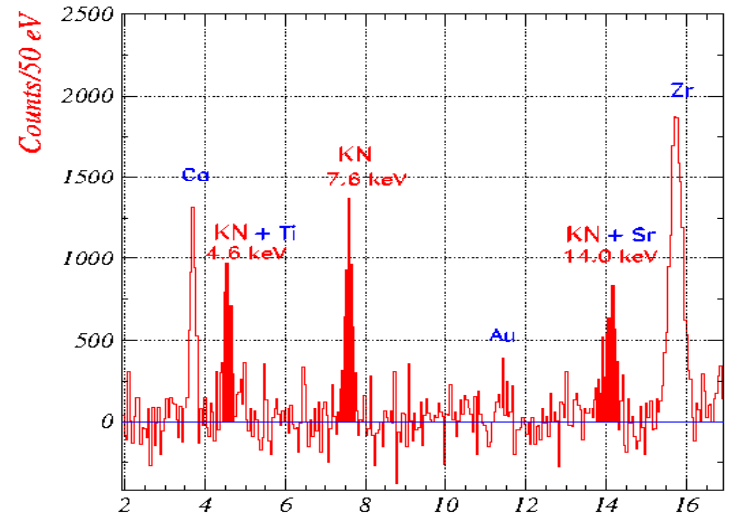


# Some results of DEAR and VIP obtained with CCD-based setups



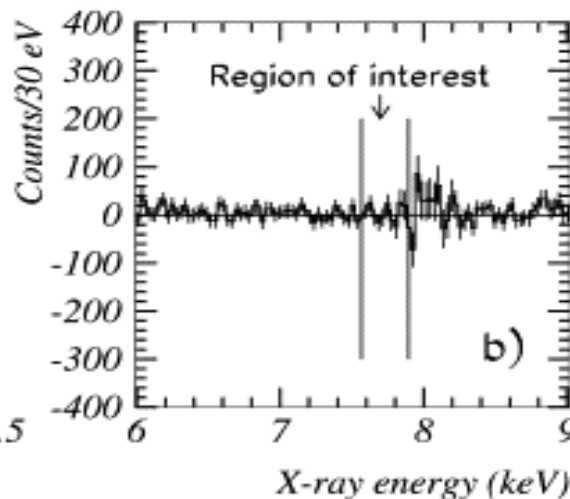
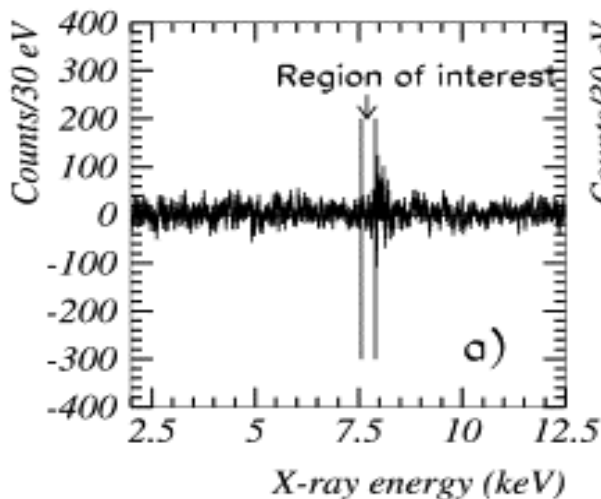
## Kaonic Hydrogen 1s transitions

G. Beer, et al. Phys. Rev. Lett. 94, 212302 (2005)



## Kaonic Nitrogen yields

T. Ishiwatari, et al. Phys. Lett. B. 593 (2004)



## Limit on the violation of Pauli exclusion principle

S. Bartalucci et al., Phys. Lett. B 641 (2006)

E. Milotti et al., Int. J. of Modern Physics A Vol. 22, Nos. 2 & 3 (2007)

# *Are CCDs completely superseded by CMOS?*

general opinion: "it's complicated" (Teledyne)

## CCDs

analog output

**slow** (serial, max 4 nodes) readout  
fast models deliver also direct column  
output but require 1 channel/column  
other workaround is storage area

almost 100% active area

**uniform response**  
(suitable for direct spectroscopy)

high sensitivity, low output node  
capacitance and single dedicated  
amplifier

**high depletion** up to fully depleted

**Global Shutter**

**high system cost**

## CMOS

digital output

**fast** (single pixel) readout

part of area used by on-chip el.

**individual pixel response**  
(not suitable for direct spectroscopy)

high sensitivity at the cost of **increased  
noise**, local (limited) amps & ADCs

**depletion typically limited** to 10  $\mu\text{m}$

**Rolling Shutter**

**low cost** (higher integration)

Comment: new technologies emerge in between (CMOS+drift field), based on novel wide bandwidth semiconductors (HgCaTe:As on HgCaTe), sensitive from soft X-ray to 5.5  $\mu\text{m}$ . Currently very expensive (James Webb telescope), but directed towards market products.

# *New proposals based on CCD development at LNF*

Reanalysis of VIP data in a DAMIC-like frame:

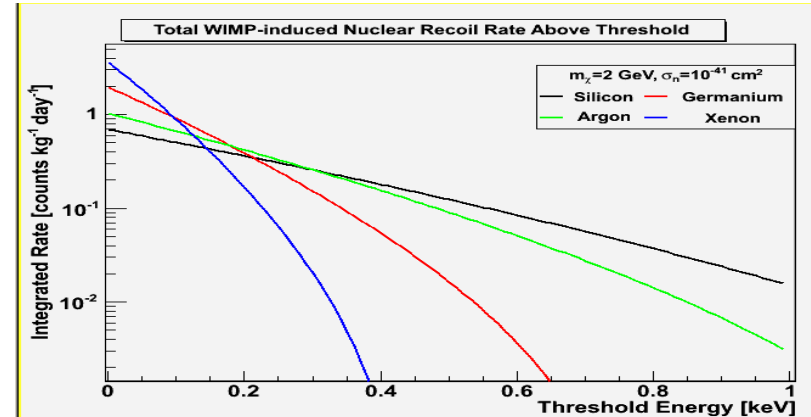
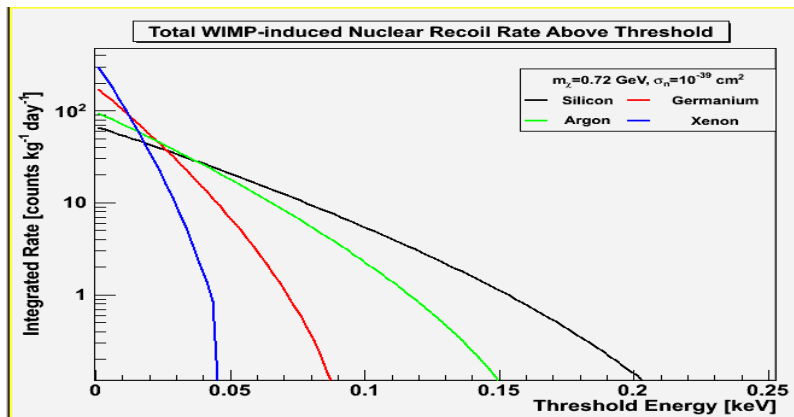
Vip CCDs have a much thinner depletion ( $\sim 25\text{-}30\text{ }\mu\text{m}$ ) than DAMIC ones ( $450\text{ }\mu\text{m}$ ), but VIP has a long period of DAQ (775 days), a better single pixel discrimination and a large area ( $117\text{ cm}^2$ ). Considering the charge collection for clusters occurs with good efficiency also in the "free/low" field region, as demonstrated by our 2-pixel analysis and supported by the Gregory Prigozhin et al. IEEE Tr. on Electron Devices, V. 50, 1, 2003, we can count on a total exposure up to  $2.1\text{ kg} \cdot \text{day}$  (7.8 larger than DAMIC publication).

Still, we have to lower ( $\sim 100\text{ eV}$ ) the minimum threshold (currently  $250\text{-}300\text{ eV}$ ), by taking advantage of the very large number of images acquired,  $\sim 400000$ , allowing to define a pedestal for each of the 22 Mpixels, data not available for long-exposure experiments.

An algorithm for increasing the cluster identification/classification from 2 to 9 pixels has already been developed.

Many steps are still required, while DAMIC prepares the next two phases (100g and 1 Kg detectors). Other experiments (SENSEI) also published a result for  $48\text{ g} \cdot \text{day}$  in March 2021; upgrades are coming.

Possible VIP setup sensitivity was identified in the (uncovered)  $0.5\text{ - }1.8\text{ GeV}$  range.



# SPHYNX

(Structure Probing by Holographic Imaging at Nanometer scale with X-ray lasers)

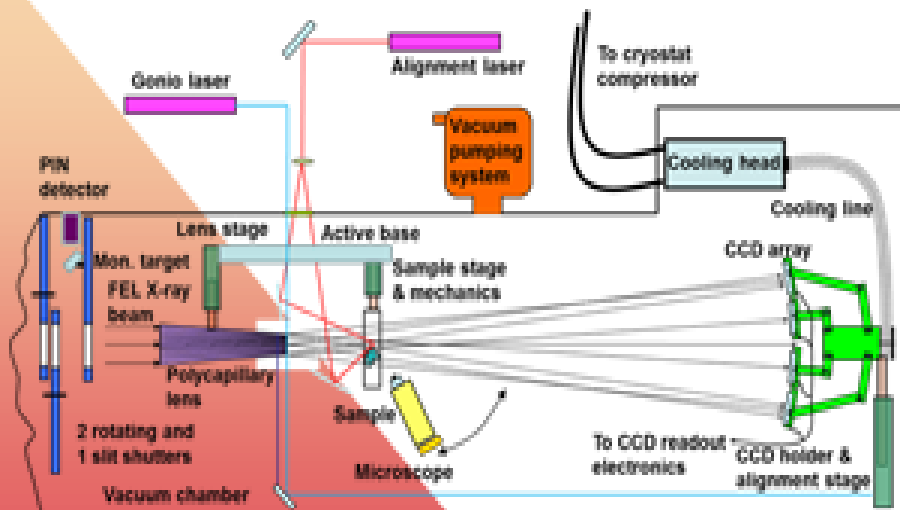
The Idea is to produce X-ray phase-contrast holograms of microscopic samples and of their internal parts with nanometer resolution using a combination of polycapillary lenses, large X-Ray CCD arrays and XFEL sources. The proposed configuration allows beam splitting, focusing, magnification and refractive diffraction in the keV range.

It could have applications in cellular biology, nanorobotics, 3D circuitry.

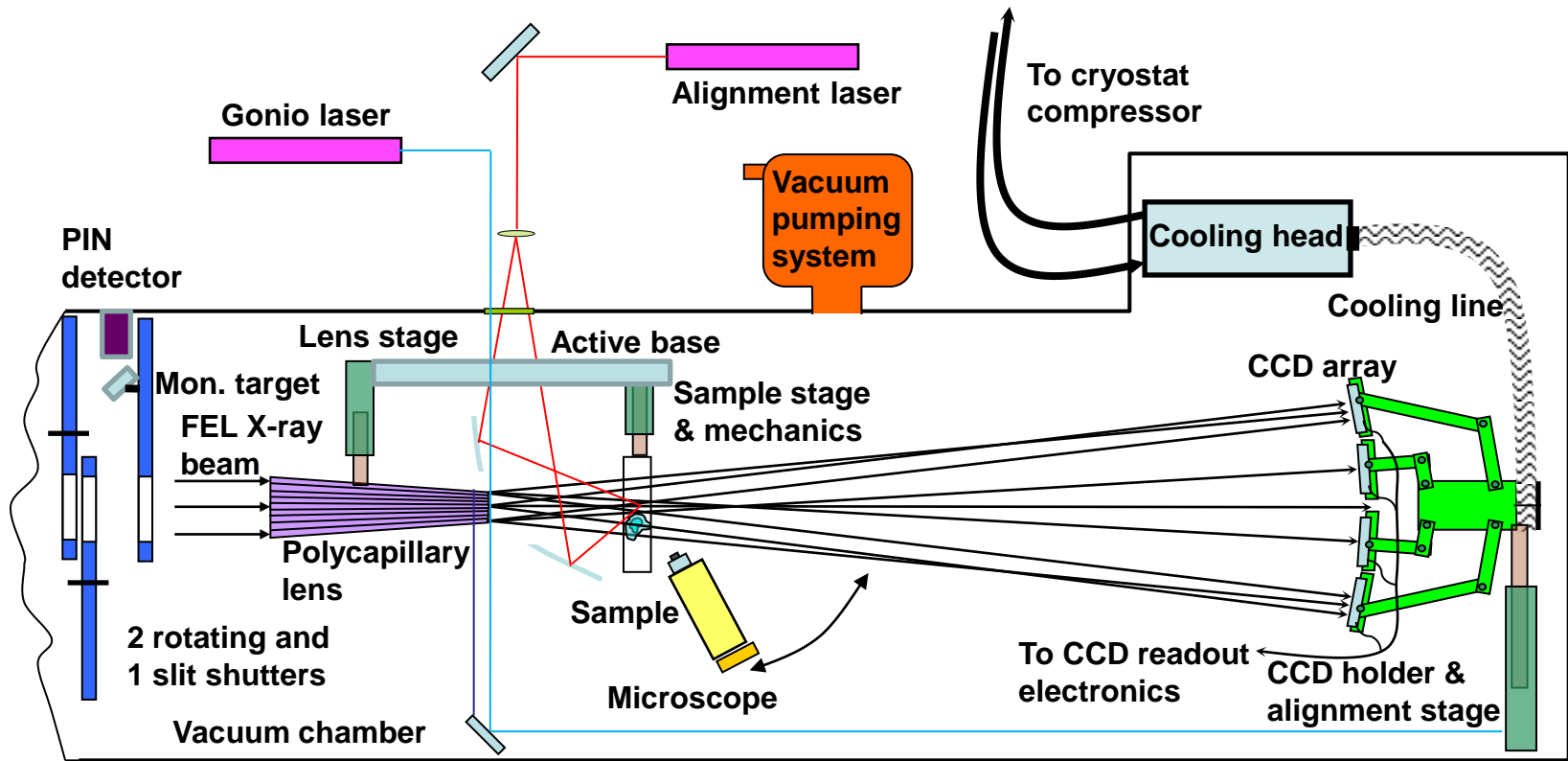
Our project is coordinated by INFN and the partners are ARTEL S.R.L.

We plan to liaise with Research Infrastructure (European X-FEL, PSI Synchrotron, DIAMOND)

Contact email [Mihai.Iliescu@Inf.infn.it](mailto:Mihai.Iliescu@Inf.infn.it)



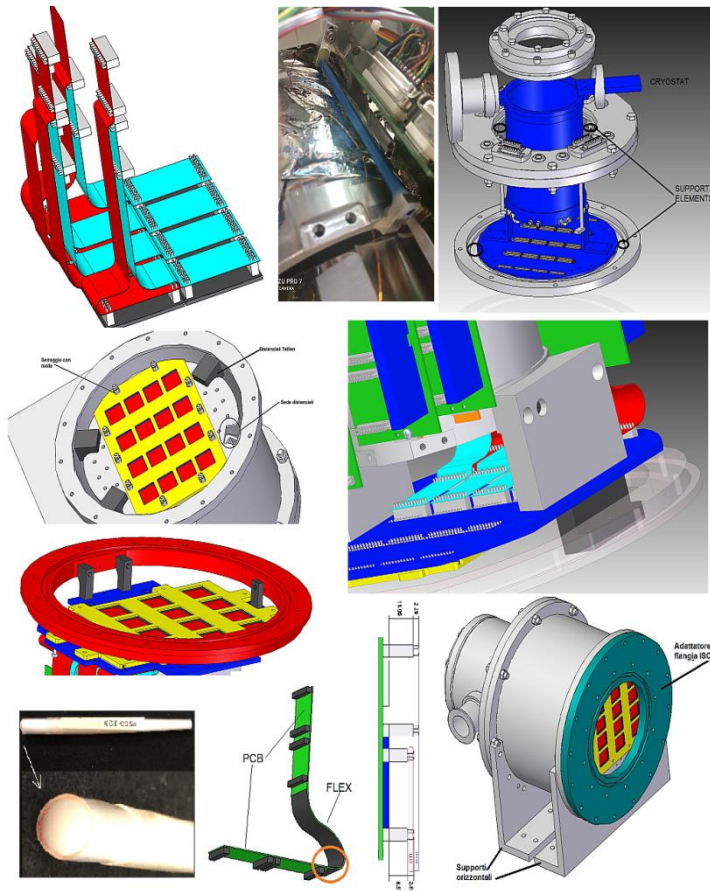
## CCD-based XRH setup layout



The project aims realizing a soft X-ray holography apparatus for phase contrast imaging, based on a large area CCD array and new X-ray optics, to be used on the recently available XFELs. The XFEL beam will grant three of the critical parameters, namely the coherence, the ultra-short exposure and the requested flux. The large area deeply depleted CCD array will ensure the full coverage of the useful solid angle, while the concentrated (over few  $\mu\text{m}$ ) X-ray source will be created using polycapillary optics, on which many studies demonstrated a high degree of coherent propagation. The reference beam consists in the fraction of rays not crossing the sample, overlapping the last's one shadow over the whole detector area, geometry uniquely allowed by capillary half-lenses.

# Structure Probing by Holographic Imaging at Nanometer scale with X-ray lasers (SPHINX)

SPHINX aims producing an X-ray phase-contrast holography system for imaging microscopic samples and their internal parts with nanometer resolution, using a combination of polycapillary lenses, large X-Ray CCD arrays and XFEL sources. The proposed configuration allows beam splitting, focusing, magnification and refractive diffraction in the keV range.

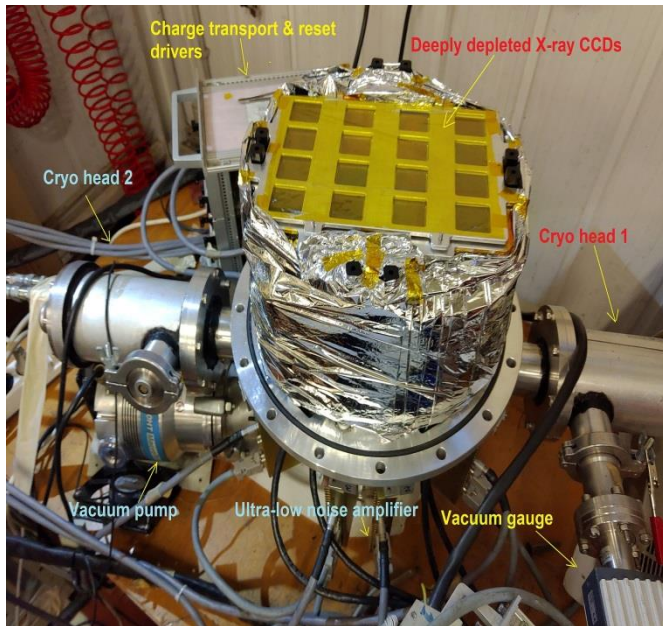


Status at the end of financed period (November 2020):

1. Full design (mechanics, cryogenics and electronics) finalized; production in advanced phase.
2. First X-ray optics delivered, synchrotron tests in preparation (waiting for mobility opening).
3. DAQ and slow control software completed. All detectors tested, fully functional.
4. MC code in advanced phase; reconstruction program work initiated
5. Calibration system under development



## Structure Probing by Holographic Imaging at Nanometer scale with X-ray lasers (SPHINX)



Update on the last period (November 2020 - January 2021):

1. Full detector assembly completed.

2 Vacuum and cryogenic testing completed.

3. Optics bench design completed, all components realized, ordered actuators arrived, second vacuum chamber and feedthrough flanges realized.

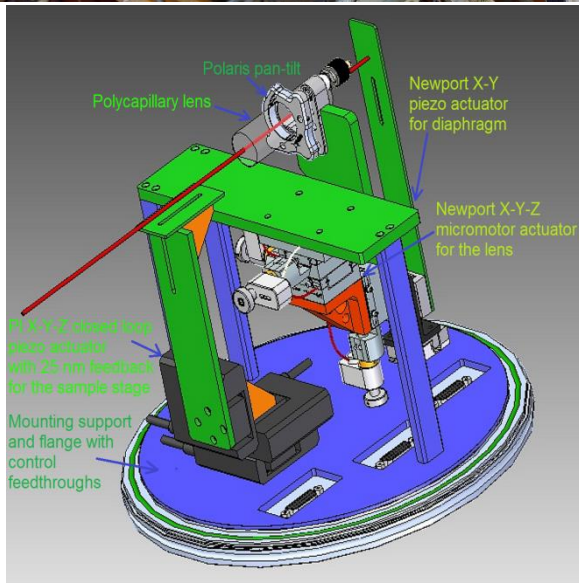
The bench parameters are:

- 10 degrees of freedom (8 translations, 2 rotations)
- 50 nanometer average precision
- 25 nm measurement feedback for the sample stage.

Installation in advanced phase.

4. Measurement plan agreed with DIAMOND synchrotron, to be started when reopening.

5. Contact with European X-FEL established, more specific plans to follow the optics investigation.



***Thank you for attention***